REPORT DOCUMENTATION PAGE

Form Approved
OMB No. 0704-0188

1. REPORT DATE *(DD-MM-YYYY)*	2. REPORT TYPE	3. DATES COVERED *(From - To)*
16-01-2003	Technical Paper	

4. TITLE AND SUBTITLE

Effect of Propellant Temperature on Efficiency in the Pulsed Plasma Thruster

5a. CONTRACT NUMBER

5b. GRANT NUMBER

5c. PROGRAM ELEMENT NUMBER

6. AUTHOR(S)

Gregory G. Spanjers, Jamie B. Malak, Robert J. Leiweke, Ronald A. Spores

5d. PROJECT NUMBER
1011

5e. TASK NUMBER
0011

5f. WORK UNIT NUMBER

7. PERFORMING ORGANIZATION NAME(S) AND ADDRESS(ES)

Air Force Research Laboratory (AFMC)
AFRL/PRSS
1 Ara Drive.
Edwards AFB, CA 93524-7013

8. PERFORMING ORGANIZATION REPORT NUMBER

AFRL-PR-ED-TP-2003-012

9. SPONSORING / MONITORING AGENCY NAME(S) AND ADDRESS(ES)

Air Force Research Laboratory (AFMC)
AFRL/PRS
5 Pollux Drive
Edwards AFB CA 93524-7048

10. SPONSOR/MONITOR'S ACRONYM(S)

11. SPONSOR/MONITOR'S NUMBER(S)
AFRL-PR-ED-TP-2003-012

12. DISTRIBUTION / AVAILABILITY STATEMENT

Approved for public release; distribution unlimited.

13. SUPPLEMENTARY NOTES

14. ABSTRACT

15. SUBJECT TERMS

16. SECURITY CLASSIFICATION OF:			17. LIMITATION OF ABSTRACT	18. NUMBER OF PAGES	19a. NAME OF RESPONSIBLE PERSON
					Leilani Richardson
a. REPORT	b. ABSTRACT	c. THIS PAGE	A		19b. TELEPHONE NUMBER *(include area code)*
Unclassified	Unclassified	Unclassified			(661) 275-5015

- 075

MEMORANDUM FOR PRS (In-House Publication)

FROM: PROI (STINFO)

16 Jan 2003

SUBJECT: Authorization for Release of Technical Information, Control Number: **AFRL-PR-ED-TP-2003-012**
Gregory G. Spanjers; Jamie B. Malak; Robert J. Leiweke; Ronald A. Spores, "Effect of Propellant Temperature on Efficiency in the Pulsed Plasma Thruster"

(Statement A)

Journal of Propulsion and Power
(July-Aug 1998 issue)

JOURNAL OF PROPULSION AND POWER
Vol. 14, No. 4, July–August 1998

Effect of Propellant Temperature on Efficiency in the Pulsed Plasma Thruster

Gregory G. Spanjers,* Jamie B. Malak,† Robert J. Leiweke,‡ and Ronald A. Spores§
U.S. Air Force Research Laboratory, Edwards Air Force Base, California 93524

A pulsed plasma thruster (PPT) benefits from the inherent engineering simplicity and reduced tankage fraction gained by storing the propellant as a solid. The solid is converted to the gaseous state and accelerated by an electric discharge across the propellant face. Previous research has concluded that as little as 10% of the consumed propellant is converted to plasma and efficiently accelerated. The remaining propellant is consumed in the form of late-time vaporization and particulate emission, creating minimal thrust. Critical to improving the PPT performance is improving the propellant utilization. The present work demonstrates one possible method of increasing the PPT propellant efficiency. By measuring the PPT thrust, propellant consumption, and propellant temperature while varying the power level, duration of the experimental run, and total propellant mass, a correlation is established between decreased propellant temperature and increased propellant efficiency. The method is demonstrated by performance measurements at 60 W and 5 W, which show a 25% increase in thrust efficiency, while the propellant temperature decreases from 135 to 42°C. Larger increases in the efficiency may be realized on-orbit where operating temperatures are commonly subzero. The dependence of propellant consumption on temperature also creates systematic errors in laboratory measurements with short experimental runs, and orbit analyses where the PPT performance measured at one power level is linearly scaled to the power available on the spacecraft.

Nomenclature

A = cross-sectional area of propellant
C_P = specific heat, 1200 J/kg °C for Teflon®
F = thrust, N
f = pulse frequency, Hz
g = gravitational constant, 9.81 m/s^2
k = thermal conductivity, 0.167 W/m °C for Teflon
L = diffusion length, m
I_{sp} = specific impulse, s
M = total propellant consumed, kg
M_{prop} = total mass of the propellant sample
$\dot{m}$ = propellant flow rate, kg/s
m = propellant consumed per discharge, kg
N = number of discharges
n = number of experiments
P = input power, W
Q_0 = heat flux at propellant face, W/m^2
R = fit parameter
S = sample variance
T = temperature, °C
t = time, s
z = axial distance from propellant face
η = efficiency
ρ = density, 2152 kg/m^3 for Teflon
Φ = fit of M, N

Received Sept. 18, 1997; revision received Jan. 9, 1998; accepted for publication Feb. 17, 1998.

*Group Leader, Electric Propulsion Laboratory, Propulsion Directorate, OLAC AFRL/PRRS. Member AIAA.

†Electronics Engineer, Propulsion Directorate, OLAC AFRL/PRRS.

‡Researcher, AFOSR Graduate Summer Research Program, Propulsion Directorate, OLAC AFRL/PRRS; currently at Ohio State University, Dept. of Aerospace Engineering, Engineering Mechanics, and Aviation, 2036 Neil Avenue Mall, Columbus, OH 43210. Member AIAA.

§Chief, Spacecraft Propulsion Branch, Propulsion Directorate, OLAC AFRL/PRRS. Member AIAA.

I. Introduction

THE pulsed plasma thruster (PPT)[1] is an attractive propulsion option for small, power-limited satellites. The PPT, shown schematically in Fig. 1, operates at low power levels (<100 W) by charging an energy-storage capacitor on a long time scale (1 s), and then discharging on a short time scale (10 μs) at high instantaneous power. High reliability is achieved through the use of a solid Teflon propellant that eliminates the engineering complexity associated with gaseous propellants. The only moving part on the PPT is a spring that passively feeds the propellant. The solid propellant is converted to vapor and partially ionized by an electric discharge across the propellant face. Acceleration is accomplished by a combination of thermal and electromagnetic forces to create usable thrust. The inherent engineering advantages of the PPT design have enabled the thruster to complete several space missions over the past 30 years with no failures.[1–3]

Two primary features that make the PPT attractive for small power-limited satellites are the solid propellant and the integrated capacitor. The solid propellant allows significant reductions in the thruster mass and volume by eliminating the propellant tankage and valves. In addition, the solid propellant is nontoxic and not pressurized, making the PPT compatible with Space Shuttle Bay requirements. The capacitor enables the PPT power level to be changed by varying the discharge frequency. For example, a PPT optimized for a discharge energy of 20 J can be operated at 20 W using a 1-Hz discharge frequency, or at 0.2 W using 0.01 Hz. In this manner, the PPT can be operated at the very low power levels available on small satellites.

The problem with the PPT is poor performance. The last flight-qualified design,[4] for the LES 8/9 satellite, and operating at 20-W power supplied to the PPT, achieved a thrust of 300 μN, a specific impulse of 1000 s, and a thrust efficiency of 8%. The potential for significant improvement in PPT performance has fueled research dedicated to understanding the basic

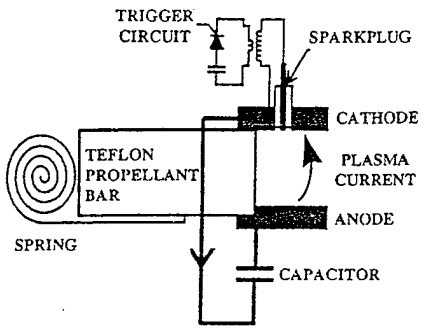

Fig. 1 Schematic diagram of the PPT.

physics of the device. The increased understanding can then be used to design future PPTs that possess significantly improved performance while maintaining the inherent engineering robustness.

Previous PPT research[5,6] showed the existence of a high-velocity plasma (~40 km/s) and a slower neutral component (~3 km/s) in the discharge. An important open question that remained was whether a significant portion of the thrust was a result of neutral gasdynamic pressure.[5] Estimates of the total plasma mass from charge collector measurements indicated that all of the thrust could be accounted for by the fast ions. Continual production of neutral vapor, after the capacitor energy dissipated, was then hypothesized to reconcile the measured propellant consumption rate. A detailed measurement of the PPT exhaust components and their energy distributions is required to conclusively resolve this issue. Further research investigated electrode configurations designed to increase the thrust because of gasdynamic plasma expansion relative to the thrust generated by accelerating the plasma electromagnetically.[7] Recent measurements directly measured the late-time vaporization of the neutral gas from the propellant face and confirmed the earlier hypothesis.[8] The high-density neutral vapor presumably exhausts near the sound speed associated with the boiling temperature of Teflon (~300 m/s), producing minimal thrust. The research also identified that particulate emission from the thruster is a significant propellant loss mechanism, consuming as much as 40% of the propellant while producing negligible thrust.[9]

The present research shows that influences that cause the PPT propellant temperature to decrease cause an accompanying decrease in the propellant consumption rate, with no decrease in the thrust. Influences directly shown to affect operating temperature and propellant consumption are firing duration, power level, and total propellant mass. This indicates that operation at the lower temperature has significantly higher propellant efficiency, thrust efficiency, and specific impulse.

This finding has significant implications for laboratory PPT research, PPT-satellite integration, and the development of next-generation PPTs. If not characterized and accounted for in the analysis, a transient phase observed when the PPT is first energized will cause systematic errors in the measurement of the propellant consumption rate and the calculations of specific impulse and thrust efficiency. Total propellant mass is also shown to affect laboratory measurements, with smaller propellant samples achieving a higher temperature and propellant consumption rate.

For satellite integration, the thermal design of the satellite becomes a factor in PPT performance. A thermal interface resulting in elevated PPT temperatures will require additional propellant to complete the mission. Conversely, a thermal design that acts to cool the PPT will result in significant propellant mass savings.

The most significant impact of the present work is on the development of next-generation PPTs. These results mark the first success at reducing the propellant consumption rate without decreasing the thrust. This indicates that the propellant savings is in the form of reduced late-time vaporization or particle formation, because these components of the exhaust contribute minimally to the total thrust. Future designs can achieve increased propellant efficiency, and associated increases in thrust efficiency and specific impulse by increasing the passive heat transfer away from the PPT propellant.

II. Experimental Apparatus

The experiments are performed at the U.S. Air Force Research Laboratory in the Electric Propulsion Laboratory. Propellant consumption and temperature measurements are performed in chamber 5, which is 1.2 m in diameter and 1.8 m in length. Typical base pressures of 3×10^{-5} torr are achieved using a 1400-l/s turbomolecular pump. Thrust measurements are performed in chamber 2, which is 2.4 m in diameter and 3.0 m in length. Typical base pressures of 2×10^{-5} torr are achieved using two 17,500-l/s diffusion pumps.

A. Pulsed Plasma Thruster XPPT-1

The experiments are conducted using XPPT-1 (Experimental Pulsed Plasma Thruster #1). The XPPT-1, shown in Fig. 2, is similar to the LES 8/9 PPT[4] electrically and geometrically; however, diagnostic access has been increased in the XPPT-1 design by removing the housing around the electrodes.[8,9] In the present work testing was performed using both 20- and 17-μF capacitors. For the 20-μF configuration the interface between the energy storage capacitor and the stripline has been modified in XPPT-1 to allow for a Rogowski coil (Ion Physics CM-1-L) that measures the discharge current. This modification adds approximately 70 nH to circuit inductance. The 20-μF configuration was used principally for the propellant consumption and temperature measurements. The 17-μF configuration, using an original capacitor from the LES 8/9 PPT, was used for the thrust measurements because it has a lower mass than the 20-μF configuration (4.1 vs 13.6 kg). This increases the thrust-to-weight ratio for a more accurate thrust measurement.

B. Diagnostics

1. Thrust Stand

The stand is a duplicate of the torsional thrust stand developed at NASA-LeRC.[10] With XPPT-1 configured for 17 μF affixed to the thruster platform, the natural oscillation frequency is 0.14 Hz (7.3 s/period) with a decay time constant of 36.5 s. The oscillation damping is significantly greater than that reported from the identical thrust stand at NASA-LeRC.[10] The increase is attributable to cable connections from the laboratory power supplies to the thrust stand. Removing the cables reduces the oscillation decay to approximately that reported in Ref. 10. Calibration is performed as described in Ref. 10, although with a set of five weights between 5 and 15 mg.

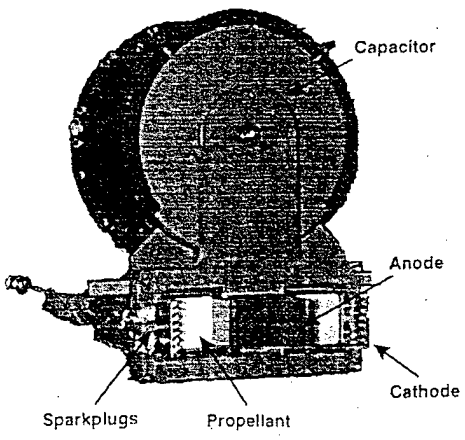

Fig. 2 XPPT-1 with major components identified.

There are three main sources of measurement uncertainty in the thrust measurement: 1) Random measurement uncertainty of the thrust-stand displacement in response to the calibration weights, 2) random measurement uncertainty of the thrust-stand displacement in response to the PPT thrust, and 3) systematic uncertainty in correlating the oscillating displacement signal to the true thrust. Uncertainties 1 and 2 are characterized by comparing several displacement measurements of the same applied force and calculating the standard deviation. Although these are recalculated for each set of thrust measurements, a typical test at 256 μN has a calibration measurement uncertainty of 10.2 μN (4.0%) and a thrust measurement uncertainty of 6.7 μN (2.6%). These combine to give an overall measurement uncertainty of 12 μN (4.7%). In the present work the thrust measurement uncertainty is always between 4 and 5%.

Uncertainty 3 results from the thrust-stand displacement in response to the PPT firing consisting of a small-amplitude oscillation around a much larger displacement (typical raw data can be found in Ref. 10). The small-amplitude oscillation is at the PPT firing frequency and has increased amplitude as the pulse frequency is decreased. Although the problem of correlating the observed oscillatory displacement to the applied thrust is analytically tractable, for this analysis the mean value of the small-amplitude oscillation is used for the thrust stand displacement. This is a systematic measurement uncertainty that is ignored in the present work. In the worst-case scenario, where the small-amplitude oscillation is treated as an independent random measurement uncertainty, this creates an additional measurement uncertainty of 8.5 μN. Using the preceding example, the total thrust measurement uncertainty increases to 14.9 μN (5.8%).

The baseline displacement of the thrust stand will tend to drift over time, presumably a result of mechanical stresses on the experimental chamber under vacuum and thermal effects. The rate of drift is largest immediately after the chamber is evacuated and continues to decrease over time. During testing, the thrust-stand displacement caused by drift is typically 10% of the total displacement during calibration. By using a baseline with a slope equal to the drift rate, and by performing several calibrations, the measurement uncertainty is reduced to the value near 4% previously quoted. During thrust measurements, the baseline drift is recorded by periodically turning the thruster off for a few seconds. The thrust-stand displacement is measured from a drifting baseline drawn between these points.

2. *Propellant Consumption*

Propellant consumption is measured by weighing a propellant test sample before and after an experimental run. The test sample cross section is 2.3 × 2.3 cm. The sample length (mass) used in the present experiments varied between 1 cm (10 gm) and 5 cm (50 gm). The sample is placed in front of the existing spring-fed propellant bar in the PPT. The Precisa Balance Model 240A is self-calibrating with internal weights and has a measurement uncertainty of 0.1 mg. For experimental runs of 5000 discharges at 1 Hz and 20 J, the experimental reproducibility is typically 3.3%, determined by making several measurements and calculating the standard deviation of the propellant consumption. Because the average propellant consumption rate is 24.9 μg/discharge, the measurement uncertainty associated with the experimental reproducibility dominates over the measurement uncertainty associated with the precision balance for experimental runs greater then 140 discharges.

It is possible for changes in the concentration of absorbed water vapor within the material to appear as transients in the propellant consumption rate. Water could be removed from the material during pumping in the vacuum chamber. After the experimental run, if the propellant was weighed before the water vapor had sufficient time to be reabsorbed, the measurement of total propellant consumed would be systematically high. Normalizing to the number of discharges during the run would result in the appearance of a transient propellant consumption rate that is initially higher than the steady-state rate. To characterize this effect a 20.6-gm propellant sample was placed in the vacuum chamber at 3×10^{-5} torr for 3.5 h. Without firing the PPT, the sample propellant mass decreased by 0.47 mg. For experimental runs greater than 570 discharges this mass is less than the 3.3% measurement uncertainty of the experiment. A second hygroscopic effect that can occur is that at elevated temperatures the propellant could lose its water content more efficiently. Thus, at the higher propellant temperatures observed at higher-power operation, a measured increase in the propellant consumption could be attributable to a decrease in the propellant water content. To characterize this effect, two 43-g propellant samples were tested during experimental runs. In one case the PPT was operated for 9600 discharges at 50 W (2.5 Hz). In the second case the PPT was operated at 20 W (1 Hz) for 8600 discharges. Temperature measurements presented in a later section show that the propellant temperature rise is near 110°C in the first case, and 50°C in the second case. Upon removal from the chamber, each propellant sample gained approximately 1 mg of mass in the first hour and then remained constant for the duration of the 30-h test. Thus, the accuracy of the PPT propellant mass measurement can be increased by waiting for 1 h after the end of the experiment prior to weighing the sample. This practice was not followed in the present work. For experimental runs greater than 1200 discharges this mass change is less than the 3.3% measurement uncertainty of the experiment.

3. *Propellant Temperature*

Propellant temperature is measured by inserting Omega K-Type Thermocouples (1.6 mm diameter) directly into the Teflon propellant and recording the temperature while the PPT is firing. The probes are inserted into four 1.6-mm-diam holes drilled from the back of the fuel bar face to depths 1, 6, 13, and 26 mm from the front face of the propellant sample. Thermal joint compound (k = 0.735 W/m °C) is injected into the holes. The thermocouples are inserted and held in place using silicone RTV adhesive sealant. The measurement uncertainty is ±2.2°C with a response time of 0.26 s. An OCTA-SCAN Model OS-367 pyrometer scans the four probes at 2.5 s/channel and displays the temperature with a resolution of ±1°C. Propellant consumption data from experimental runs with thermocouples inserted are not used because the thermal compound, RTV sealant, and the act of inserting the probes can greatly increase the measurement uncertainty.

The thermocouples are used to measure the axial temperature distribution within the propellant sample; however, they cannot physically be placed at the same radial location. Instead, each is offset from the centerline by 3.2 mm. To characterize this approximation a fuel bar was fabricated with holes at equal 1-mm depths, but displaced in a straight line across the propellant face 0, 4, 7, and 10 mm from the centerline. With the probe array orientated parallel to the electrodes, after 1500 discharges at 40 J, 1 Hz, all four probes measure the same temperature increase of 38°C. Orientated perpendicular to the electrodes the probes from the centerline to the propellant edge measure temperature rises of 42, 40, 40, and 44°C, respectively. Within the 3.2 mm offset from centerline used in the axial probe array, no variation in temperature is observed within the accuracy of the thermocouples. Although other factors, such as the quality of the thermal contact, exact axial position of the probes, and experimental reproducibility of the PPT performance act to increase the overall measurement uncertainty, the ±2.2°C accuracy of the thermocouple sensors appears to be the dominant source of experimental uncertainty in the temperature measurements. The slightly higher temperature near the electrodes may indicate that the electrodes act as a heat source to the propellant; however, this cannot be concluded within the measurement uncertainty.

When all four thermocouple probes are inserted, the high thermal conductivity of the steel thermocouple cladding (k = 1.6 W/m °C) compared to the Teflon makes it possible for the probes themselves to act as axial heat-conducting paths within the propellant. For probes positioned farther from the propellant face, this would cause a systematically high-temperature measurement error compared to what would have been measured with a single probe. To characterize this effect a single probe was inserted into the propellant sample at the second position from the propellant face (6 mm). Two experimental runs of 10,000 discharges were performed at 40 J, 1 Hz and compared to similar data where all four thermocouples were installed. The measured temperatures from the three experimental runs were found to agree within the ±2.2°C measurement uncertainty, indicating that the presence of the thermocouples within the propellant bar is not significantly perturbing the heat conduction.

III. Theory

A. Thrust Efficiency and Specific Impulse

In electric propulsion thrusters using gaseous propellants, the propellant flow rate, input power, and thrust are all monitored in real time. The specific impulse and thrust efficiency are calculated as

$$I_{sp} = F/\dot{m}g, \qquad \eta = F^2/2\dot{m}P$$

For PPT testing the thrust is measured in real time, but there is an inherent inability to measure the propellant consumption during the experimental run. Instead a discharge-averaged propellant consumption is measured, which is the total propellant consumed in the experimental run normalized to the number of discharges. The following equations are then used to calculate the specific impulse and thrust efficiency:

$$I_{sp} = F/f(M/N)g, \qquad \eta = F^2/2f(M/N)P$$

B. Statistical Analysis of the Propellant Consumption Rate

A regression analysis is used to fit the data from i-independent experimental measurements of the total propellant consumed M_i, to the number of discharges in the experiment N_i, and create the least-square-fit, $M = \Phi(N)$. The propellant consumption rate m (mass/discharge), is calculated as $m = [d\Phi(N)/dN]$. The uncertainty in the propellant consumption rate is calculated as

$$\Delta m = S_M/S_N\sqrt{n-1}$$

where the sample variances in M and N are

$$S_M^2 = \frac{1}{n-2}\sum_{i=1}^{n}[M_i - \Phi(N_i)]^2$$

$$S_N^2 = \frac{1}{n-1}\left\{\sum_{i=1}^{n} N_i^2 - \left[\left(\sum_{i=1}^{n} N_i\right)^2 \Big/ n\right]\right\}$$

The R^2 value of the fit, which describes what fraction of the variations in the measured M is attributable to variations in N, is calculated as

$$R^2 = 1 - \frac{\sum_{i=1}^{n}(M_i - \Phi(N_i)^2}{\sum_{i=1}^{n}(M_i - \bar{M})^2}$$

where $\bar{M}$ is the mean value of the n data points. The uncertainty in the y intercept of the least-squares-fit is calculated as

$$\Delta y_{\text{intercept}} = S_M\sqrt{\frac{1}{n} + \frac{(\bar{N})^2}{(n-1)S_N^2}}$$

C. Temperature

The heat conduction within the propellant bar is described by

$$\nabla^2 T = \frac{k}{\rho C_P}\frac{\partial T}{\partial t}$$

To simplify the boundary conditions three assumptions are made. First, heat flow is assumed to be one-dimensional conducting only in the axial direction. This neglects heat conduction to the electrodes, an approximation supported by the measured temperature increase toward the electrodes of only 4°C, which is within the measurement uncertainty. Second, the discrete energy pulses from the PPT discharge are assumed to be equivalent to a steady-state heat flux on the propellant surface. This is justified by the low thermal diffusivity of the Teflon. For a 1-Hz PPT pulse frequency, the characteristic distance for heat conduction between pulses, which is expected to be equal to the wavelength of perturbations in the temperature profile caused by the discreet pulses, is

$$L = \sqrt{(kt/\rho C_P)} \cong 250\ \mu\text{m}$$

This perturbation wavelength is not resolvable within the 1.6-mm spatial resolution of the thermocouple probes. Third, the propellant bar is assumed to extend infinitely in the axial direction. This approximation is expected to be valid because of the poor thermal conductivity of the Teflon that would prevent significant heat from reaching the rear interface of the propellant sample. Using these assumptions the heat equation is solved to give the relationship between heat flux at the surface and axial temperature distribution within the propellant

$$T(z) - T_i = \frac{2Q_0}{kA}\sqrt{\frac{kt}{\pi\rho C_P}}\exp\left[-\frac{\rho C_z^2}{4kt}\right] - \frac{Q_0 z}{kA}\left(1 - \text{erf}\sqrt{\frac{\rho C_P z^2}{4kt}}\right)$$

IV. Experimental Results

A. Transient Effects

These measurements characterize the dependence of the propellant consumption and temperature on the duration of the experimental run. To measure the propellant consumption, the propellant sample is weighed and inserted into the PPT, the chamber is pumped down, and the specified number of discharges are performed. The chamber is returned to atmospheric pressure, the propellant sample removed, and reweighed. The duration of the experimental run is varied in a random fashion to preclude a systematic error in the analysis attributable to the evolution of the propellant fuel face over the course of the entire experiment. Prior to any of the experimental runs, the propellant sample had been used in over 10,000 discharges so that a slightly concave shape had been eroded into the face.

Figure 3 shows the propellant consumption dependence on the number the PPT discharges. For Fig. 3 XPPT-1 was configured with 20 μF and discharged at 1-Hz frequency with a discharge energy of 20 J (20 W). For this case, the propellant sample was cleaned with emory paper and methanol to remove any darkened areas created in the previous experimental run without altering the concave shape eroded into the front face. This is the only data set presented where the propellant sample

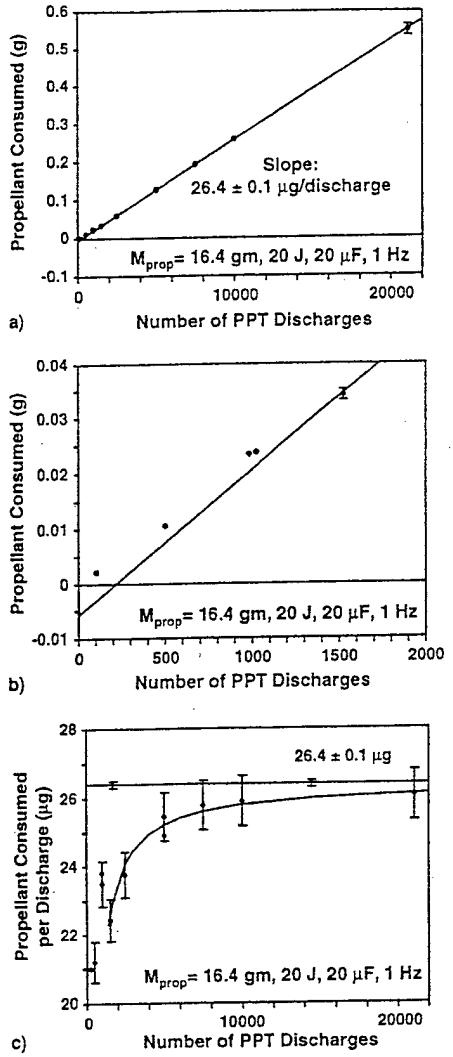

Fig. 3 Propellant consumption characteristics at 20 J, 20 W: a) total propellant consumed as a function of the duration of the experimental run, b) data from a) on an expanded scale to show the transient behavior occurring for $N < 1500$, and c) data from a) normalized by N to give the discharge-averaged propellant consumption per discharge.

was cleaned. The same data are plotted in Fig. 3 in a manner to illustrate different features. Figure 3a shows 11 measurements of M for a varied number of PPT discharges, along with a least-squares-fit of the data from $N = 1500$ to 22,000. Error bars are smaller than the data-point symbol unless explicitly shown on the graph. The steady-state propellant consumption rate is calculated from the slope of the least-squares-fit as 26.4 ± 0.1 μg/discharge. Figure 3b shows the same graph expanded between $N = 0$ and 2000. In Fig. 3b it is apparent that the data points for experimental runs shorter than $N = 1500$ fall consistently above the least-square-fit. The propellant consumption rate during the initial 1500 discharges, which would be calculated from the slope of a line connecting these points, is significantly lower than the steady-state rate. The choice of including only data from $N > 1500$ in the regression analysis was not arbitrary. The analysis was performed on every group of data in which the lesser values were successively excluded, to determine which subset had the lowest value of R^2. For $N > 1500$, the regression analysis has $R^2 = 0.9999$, indicating an extremely good fit. The y intercept of the least-squares-fit is -5.71 ± 0.48 mg. The negative y intercept is a quantitative confirmation that the propellant consumption rate is systematically lower than the steady-state rate during the initial transient phase.

Based on Figs. 3a and 3b, the transient effects in the propellant consumption are negligible after $N = 1500$ discharges, suggesting that measurements of the PPT performance are valid after this time. However, transient effects will continue to cause a systematic error in the propellant consumption measurement. This results from the thrust being measured at a single time, while the propellant consumption is averaged over all the discharges in the experimental run. Because the initial 1500 discharges have significantly lower propellant consumption, the calculated propellant usage per discharge ($m = M/N$) is systematically lower than the instantaneous propellant consumption that created the measured thrust. This results in a calculated specific impulse and thrust efficiency that are systematically high.

The significance of this effect is illustrated in Fig. 3c, where the calculated propellant consumption rate ($m = M/N$) is plotted as a function of N. In Fig. 3c, the data values and the fit are the same as those in Fig. 3a; however, the masses are now normalized by N. The solid horizontal line corresponds to the 26.4 μg/discharge steady-state propellant consumption rate. At $N = 1500$ the propellant consumption rate is measured to be 22.4 μg/discharge, whereas the instantaneous propellant consumption rate indicated by the slope in Fig. 3a is 26.4 μg/discharge. This results in a systematic error in the calculated specific impulse and thrust efficiency of

$$\Delta m/m = \Delta I_{sp}/I_{sp} = \Delta\eta/\eta = 14.2\%$$

At $N = 5000$ this systematic error decreases to a more acceptable value of 4.4%. At $N = 6800$ the systematic error decreases to 3.3%, which is within the measurement uncertainty of the propellant consumption.

Transient effects when the PPT is operated at a higher 40 J (1 Hz, 40 W) discharge energy are shown in Fig. 4. The optimal regression fit, shown in Fig 4a, is again found by using only the data points for $N > 1500$. The least-squares-fit has an $R^2 = 0.9999$ and a negative y intercept of -8.13 ± 0.094 mg. The systematic error resulting from the initial transients is 14.1% at $N = 1500$, decreasing to 3.5% at $N = 5000$. The systematic error falls below the measurement uncertainty for $N > 5300$.

Figure 5 shows propellant temperatures measured in a 45-g propellant sample during an experimental run performed at 20 J, 1 Hz (20 W). The axial location measured from the propellant face is denoted for each trace on the graph. The temperature is observed to rise as the PPT is fired, beginning to approach a steady state after 5000 discharges. Figure 6 shows the same data plotted as functions of the axial position at four times during the experimental run. Also shown in Fig. 6 is the temperature distribution predicted at these times from the one-dimensional heat equation using a heat flux at the propellant face of 0.21 W. Close to the propellant face ($z \leq 13$ mm) good agreement is observed between the measured temperatures and the temperatures predicted by the model. The temperature measurement farthest from the propellant face is consistently higher than that predicted from the model. This is probably an indication that the approximation of an infinite fuel bar is inappropriate. Heat conduction across the interface between the propellant sample and the original Teflon PPT propellant behind the sample is greatly reduced from the heat conduction that would occur for a continuous piece of propellant. The relative agreement between the model and the experimental measurements indicates that only 1% of the power supplied to the PPT (20 W) is consumed heating the propellant (0.21 W).

Figure 7 shows the thrust measured with XPPT-1 configured at 17 μF for varied number of discharges. The measured thrust is 256 ± 12 μN for the 20-J case and 224 ± 9 μN for the 17-J case. In neither case is a systematic transient effect observed for $N < 1500$, although there does appear to be an increased random measurement uncertainty. For the 20-J case the propellant consumption rate is 27.5 μg/discharge averaged

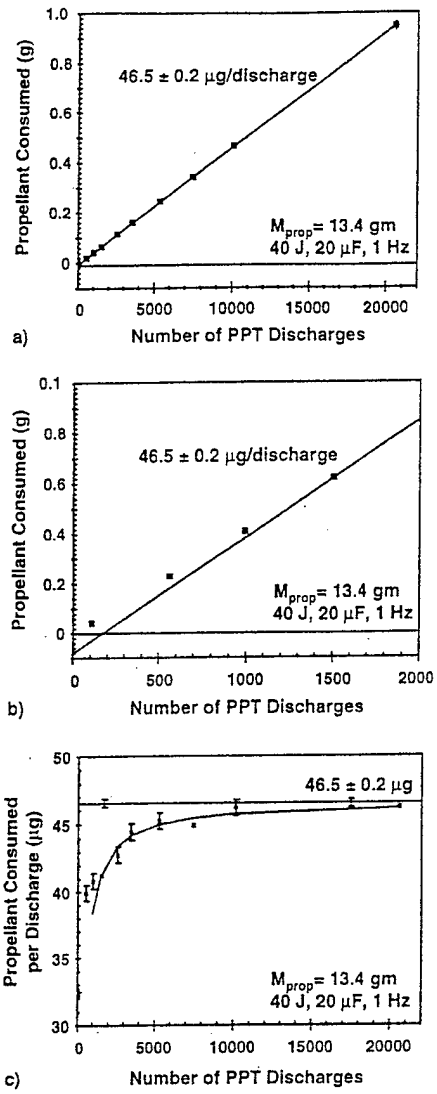

Fig. 4 Propellant consumption characteristics, similar to those shown in Fig. 3, for a 40-J discharge energy.

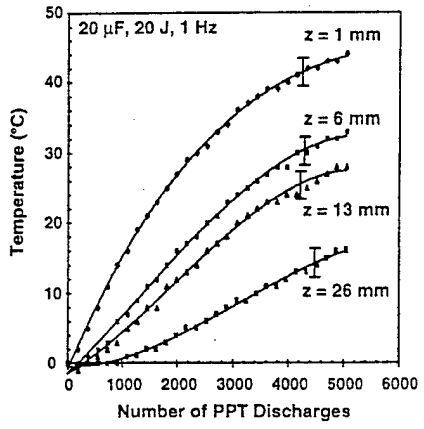

Fig. 5 Propellant temperatures at four axial locations as a function of the number of PPT discharges.

over 12,000 discharges. This results in a specific impulse of 949 ± 45 s and a thrust efficiency of 6.0 ± 0.3%. These performance parameters compare well with the performance reported for the similar LES 8/9 PPT upon which the XPPT-1 design is based.[6] The absence of a transient phase in the PPT thrust supports the conclusion that a systematic error will occur in the calculation of the PPT specific impulse and thrust efficiency because of the discharge-averaging in the measurement of the propellant consumption.

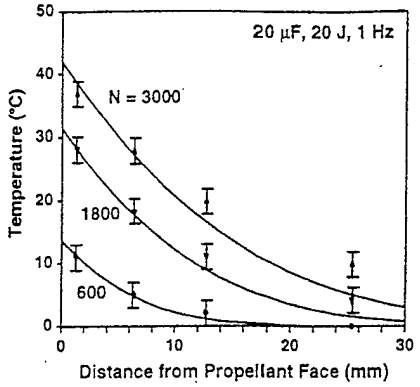

Fig. 6 Axial propellant temperature distribution at three selected times during the experimental run. The solid lines represent the temperature distribution predicted from the one-dimensional equation.

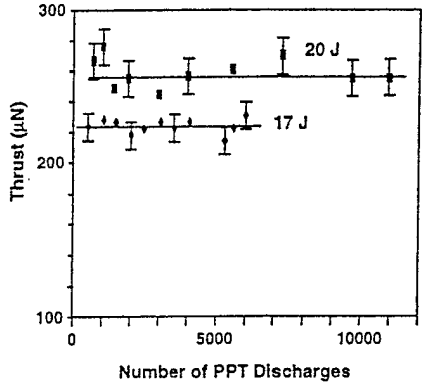

Fig. 7 PPT thrust vs number of discharges for 17 and 20 J discharge energies. In both cases the PPT was operated at a 1-Hz discharge frequency.

B. Total Propellant Mass Effects

Figure 8 shows data, collected and analyzed in the same fashion as the data from Fig. 3, for two additional cases. In these cases the propellant sample was not cleaned to ensure that the transient effect was not associated with methanol absorbed into the Teflon propellant. The two cases shown are for propellant samples of different masses: 45.3 gm (4.5 cm long) and 10.6 gm (1.0 cm long). The minimum R^2 regression fits are again found by using only the data for $N > 1500$. Both cases have good least-square-fits: $R^2 = 0.9977$ for the 10.6-gm case and $R^2 = 0.9996$ for the 45.3-gm case. More scatter and a greater uncertainty in the calculation of the slope is evident for the 10.6-gm case, which may be a result of the relatively short length of the sample. Fig. 8b shows that the initial transient effect of a lower propellant consumption rate is apparent in both cases. The y intercept in both cases is negative within the regression accuracy: y intercept = -10.4 ± 1.5 mg for the 10.6-g case and y intercept = -5.0 ± 1.3 mg for the 45.3-g case. In Fig. 8c it is apparent that the 10.6-g case has a more severe transient effect. At $N = 1500$ the systematic error for the two cases are 25.6% for the 10.6-g case and 14% for the 45.3-g case. At $N = 5000$ the systematic error is still unacceptably high: 7.7% for the 10.6-g case and 4.2% for the 45.3-g case. The 10.6-g case also requires more discharges before the measured propellant consumption rate is equal to the steady-state value within the 3.3% measurement uncertainty: $N = 11{,}600$ for the 10.6-g case and $N = 6300$ for the 45.3-g case.

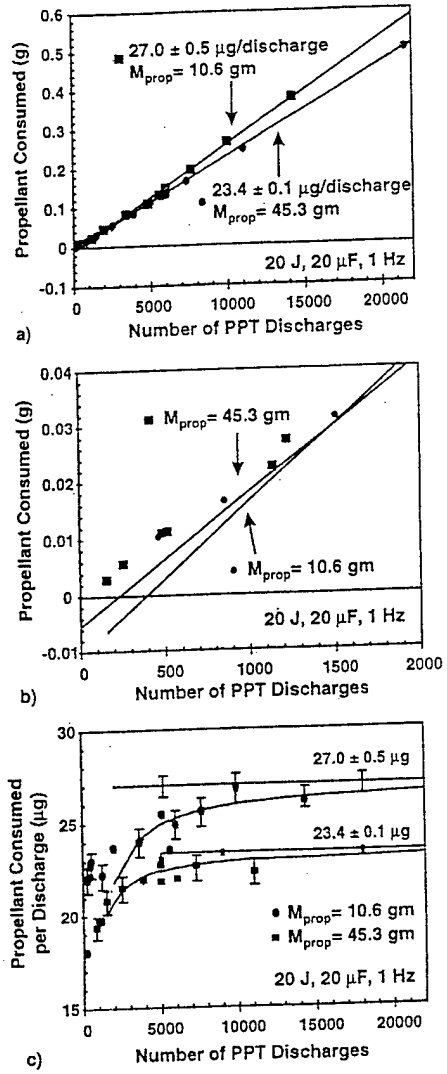

Fig. 8 Propellant consumption characteristics, similar to those shown in Fig. 3, for two propellant bars of different total mass.

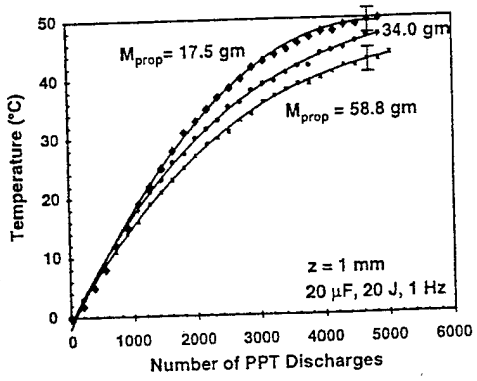

Fig. 9 Propellant temperature 1 mm behind the front face for three different propellant sample masses.

Figure 9 shows the propellant temperatures measured 1 mm behind the propellant face for three different propellant samples of different mass (varied by changing the overall length). For these measurements the PPT was operated at 20 J, 1 Hz (20 W). After 5000 discharges the propellant temperature is observed to be higher for the lower mass propellant samples. This may be a result of the finite length of the propellant sample in an effect similar to that causing the elevated temperatures at positions farther away from the propellant face in Fig. 6.

C. Power-Level Effects

The PPT power level is varied by changing the discharge frequency while keeping the discharge energy fixed. Figure 10 shows the effect on the propellant consumption rate of increasing the power level for the PPT. The PPT for these experiments was configured with 20-μF capacitance, 20-J discharge energy, and a 16-g propellant sample. To minimize transient effects, each experimental run was restricted to a duration of at least 5000 discharges and at least 1-h duration. Thus, the experimental runs at power levels of 20 W and below (1 Hz) were halted at 5000 shots and the experimental runs at 30 W (1.5 Hz) and above were halted at 1 h. A single least-squares-fit is shown for the entire power range. A 31% increase in the propellant consumption rate is observed as the power is increased from 5 W (0.25 Hz) to 60 W (3 Hz). Based on the regression fit an increase in the propellant consumption rate of 0.12 μg/discharge is expected for every watt of power increase.

Figure 11 shows the propellant temperature measured 1 mm behind the front face for the PPT operated at three different power levels. The PPT is configured with 20 μF and discharged at 20 J. Although the temperatures in the three cases initially rise together for the first 1500 discharges, they achieve significantly different steady-state temperatures. The 10-W case asymptotes to a temperature near 29°C, the 20-W case near 52°C, and the 50-W case near 111°C. Note that the majority of the temperature rise in all three cases occurs in an experimental duration shorter than that used in collecting the data on propellant consumption rate vs power level in Fig. 10. The temperature rise with power is quite linear. Using the tem-

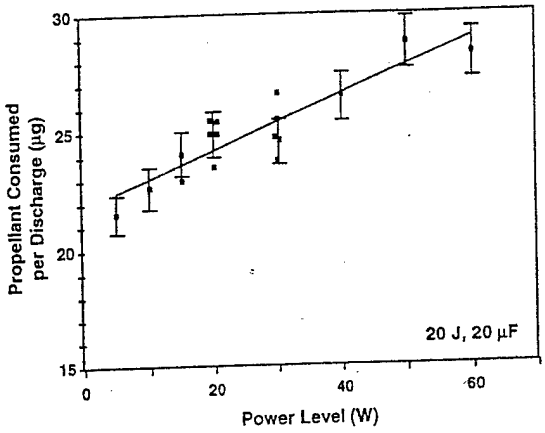

Fig. 10 PPT propellant consumption rate vs PPT power level. The discharge energy is held constant at 20 J while the discharge frequency is varied to change the power level.

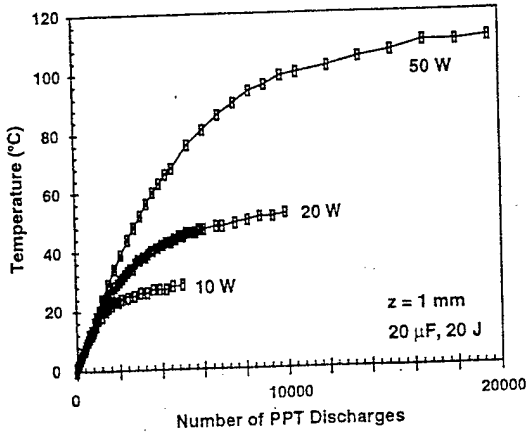

Fig. 11 Propellant temperature 1 mm behind the front face for a 20-J discharge energy and three PPT power levels.

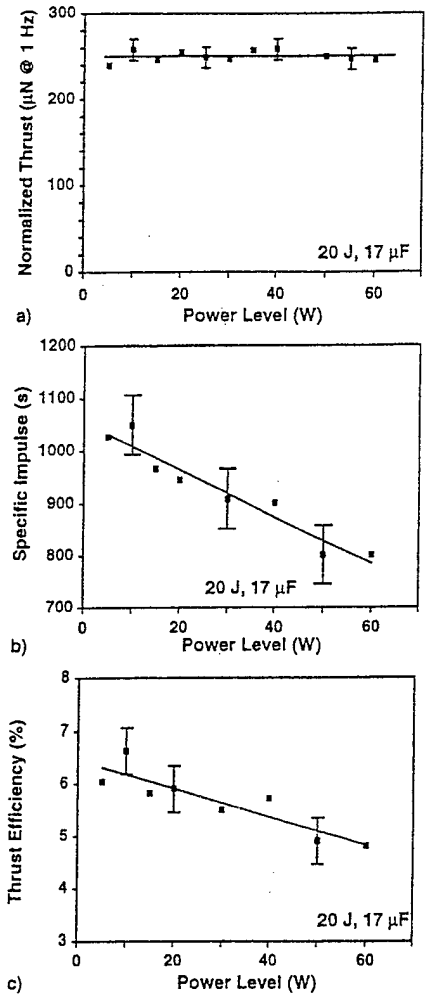

Fig. 12 Dependence of PPT performance on power level: a) normalized thrust, b) specific impulse, and c) thrust efficiency.

perature measured at $N = 5000$ in each case, a proportionality constant of 1.68 ± 0.02°C/W is found with an $R^2 = 0.9999$.

The PPT thrust, normalized to the pulse frequency, is shown in Fig. 12a. The normalization is done to show the effective thrust created per discharge for a more illustrative comparison with the propellant consumption per discharge. The PPT was configured at 17 μF and discharged at 20 J. The power was varied from 5 to 60 W by increasing the pulse frequency from 0.25 to 3 Hz. As the PPT power is increased the normalized thrust remains constant within the measurement uncertainty. As expected from Fig. 10, the propellant consumption increases significantly as the power level is increased. This results in a specific impulse that increases 28% as the power is decreased from 60 to 5 W, as shown in Fig. 12b. Similarly, the thrust efficiency increases 25% as the power level is reduced.

V. Discussion

The experimental data show three factors that result in an increased propellant consumption rate: 1) A firing duration past 1500 discharges, 2) a lower total mass (or length) propellant bar, and 3) operation at increased power. In each of these cases an increase in the propellant temperature is also measured. Although the comparison of the axial temperature distribution to the one-dimensional heat equation indicates that only 1% of the available energy is spent heating the bulk propellant, the cumulative effect of this heat over 1000 s of discharges is to cause significant increases in the propellant consumption rate. These same factors cause no observable change in the PPT thrust. The change is only observed in the propellant consumption rate and, hence, in the calculated quantities of specific impulse and thrust efficiency.

Significant changes in the propellant consumption rate with temperature, coupled with the absence of similar changes in the thrust, suggests that the decreased propellant temperatures acts to decrease the late-time vaporization.[8] This would result in a decreased propellant consumption rate, while the associated decrease in thrust would be indistinguishable within the measurement uncertainty of the thrust stand. Decreases in the particulate emission would also result in undetectable decreases in the thrust; however, a correlation between propellant temperature and propellant vaporization seems the more likely solution.[9]

Based on the early PPT research[5,6] describing a high-velocity plasma exhaust component (40 km/s) and a slow neutral exhaust component (3 km/s), a partitioning of the PPT thrust between these two components was hypothesized.[8] The present results, coupled with the long time scale of the late-time vaporization shown in Ref. 8, support the claim that the late-time neutral vapor exhausts at the low thermal velocity expected at the boiling temperature of Teflon (~300 m/s) creating negligible thrust. Coupled with the ion current measurements from Ref. 5, this strengthens the hypothesis that all of the PPT thrust is attributable to accelerated plasma. A diagnostic capable of measuring the plasma exhaust components and energy distributions, such as mass spectrometry, is needed to fully resolve this issue.

The approximation, that all of the thrust is created by the plasma exhaust component, can be used to estimate the propellant efficiency improvements with temperature. For operation at 60 W, 28.6-μg/discharge of propellant is consumed to create 256 μN of thrust at an operating temperature of 135°C. If the average plasma velocity is assumed to be approximately equal to the 40 km/s reported in the previous research,[5,6] 6.4 μg of propellant is converted to plasma to create the measured thrust. This corresponds to a propellant mass utilization efficiency of 22%. At 5-W operation, the propellant consumption has reduced to 21.6 μg as the temperature decreases to 42°C. The propellant mass utilization efficiency increases to 30% at the lower-temperature 5-W power level.

The increased propellant consumption resulting from elevated temperatures has strong implications for both the PPT researcher in the lab and the satellite designer evaluating propulsion options. For the researcher, systematic errors from the transient effect can be circumvented by taking sufficient propellant consumption data to assemble plots similar to those shown in Fig. 3. Systematic errors caused by power level effects are most effectively circumvented by performance testing at the power level to be used on-orbit. When this is impractical because of thrust-stand restrictions, the present data indicate that thrust can be measured at a different power level. Specific impulse and efficiency should be calculated from a propellant consumption rate measured, separate from the thrust measurement, at the correct power level. The most important implication for the laboratory researcher is that thermal paths away from the thruster may have a significant effect on performance. For example, a PPT thermally insulated from the surrounding chamber will operate hotter than a PPT connected to a thermally conductive mount. At the same operating conditions, the thermally insulated PPT will have an increased propellant consumption rate and decreased specific impulse and efficiency. Differences between the thermal design of experimental laboratory thrusters and the eventual flight designs also becomes a potential source of changes in performance because of temperature effects.

Because of the issues associated with the thermal design of the thruster and the thermal connection between the thruster and the chamber, other researchers should not use the present data to quantitatively determine, for example, how many discharges are required before the transient effect on propellant consumption becomes negligible. Instead, the effect should be

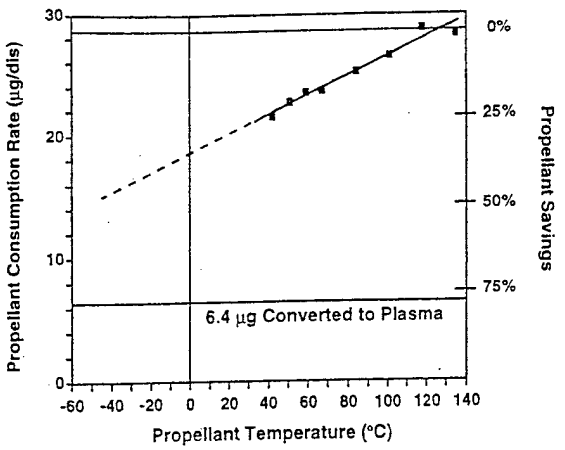

Fig. 13 Propellant consumption rate vs propellant temperature.

quantified for each thruster and experimental configuration. The purpose of the present research from an experimentalist point of view is to identify which factors are important in such a characterization.

For the satellite designer, the thermal issue increase is important. If the PPT is thermally positioned such that the satellite conducts heat to the thruster and heats the propellant, the PPT propellant consumption will increase. Conversely, a PPT thermally positioned on the satellite to minimize its temperature can realize a reduced propellant consumption rate. The potential of this effect in terms of propellant savings is shown in Fig. 13, where the propellant consumption data from Figs. 10 and 12 are plotted as a function of the propellant temperature. The dashed horizontal line at 28.6 μg represents the total propellant consumption measured at high power. The horizontal line at 6.4 μg represents the 22% of the propellant that is estimated to be converted to plasma and accelerated to high exhaust velocity. A 31% increase in the propellant consumption rate is shown as the temperature increases from 42 to 135°C. More interesting in Fig. 13 is that on-orbit spacecraft tend to operate in the temperature range from −50 to 0°C. Based on the linear extrapolation shown in the graph, the potential may exist to realize mass savings of up to 50% of the propellant. These propellant savings are not a trivial engineering problem because firing the PPT may cause substantial heating of the spacecraft.

The dependence of the propellant consumption on propellant temperature may offer an avenue to control the PPT propellant inefficiency in future PPT designs. Designs that passively cool the propellant may lead to increases in performance. Even active cooling can be considered provided the engineering simplicity of the PPT can be retained. The analysis of the temperature distribution within the propellant bar implies that only 1% of the PPT power is used heating the propellant. Redirecting a comparably small fraction of the PPT power to actively cool the propellant may be advantageous in terms of a total mass reduction of the propulsion system.

VI. Conclusions

In the present work it has been shown that influences that act to increase the propellant temperature in the PPT will also act to increase the propellant consumption rate. Principle influences demonstrated on PPT performance in the present work are the number of discharges in the experimental run, the total mass or length of the propellant bar, and the PPT power level. In each case an increase in propellant temperature resulted in an increase in the propellant consumption rate. None of these influences appeared to affect the PPT thrust. This indicates that significant improvements are attainable in the propellant efficiency by operating, interfacing, or designing the PPT to reduce the propellant temperature.

The changes in the propellant consumption rate can also lead to systematic errors in the calculation of the thruster specific impulse and thrust efficiency for short experimental runs unless the transient behavior is characterized and accounted for in the analysis. Systematic errors can also occur when PPT performance is scaled from one power level to another, and in experiments using low-mass propellant samples.

Satellite thermal designs that act to increase the PPT temperature will increase the propellant consumption rate above what is measured in the laboratory. Designs that act to keep the PPT temperature low should realize a significant savings in propellant mass.

Previous research has shown that the propellant inefficiency in the PPT to be a severe limitation on the thrust efficiency, with between 80 and 90% of the total propellant expelled at low velocity in the form of neutral gas and macroparticles. The present research is the first experimental demonstration of any control, albeit small, over the propellant consumption without adversely affecting the thrust. Scaling the present results to temperatures that may be achieved on-orbit or with active propellant cooling, illustrates the potential to significantly improve PPT thrust efficiency.

Acknowledgments

The authors wish to acknowledge input from Keith McFall and Michel Macler at the U.S. Air Force Research Laboratory, and David White of Sparta Inc. Rickie Rexroade assisted in the preparation of the manuscript. Robert J. Leiweke was funded under the U.S. Air Force Office of Scientific Research Graduate Summer Research Program.

References

[1]Guman, W. J., and Nathanson, D. M., "Pulsed Plasma Microthruster for Synchronous Orbit Satellite," *Journal of Spacecraft and Rockets*, Vol. 7, No. 4, 1970, pp. 409–415.

[2]Brill, Y., Eisner, A., and Osborn, L., "The Flight Application of a Pulsed Plasma Microthruster: The NOVA Satellite," AIAA Paper 82-1956, Nov. 1982.

[3]Guman, W. J., and Williams, T. E., "Pulsed Plasma Microthruster for Synchronous Meteorological Satellite (SMS)," AIAA Paper 73-1066, Oct. 1973.

[4]Vondra, R. J., "Flight-Qualified Pulsed Electric Thruster for Satellite Control," *Journal of Spacecraft*, Vol. 11, No. 9, 1974, pp. 613–617.

[5]Thomasson, K. I., and Vondra, R. J., "Exhaust Velocity Studies of a Solid Teflon Pulsed Plasma Thruster," *Journal of Spacecraft*, Vol. 9, No. 1, 1972, pp. 61–64.

[6]Vondra, R. J., Thomasson, K. I., and Solbes, A., "Analysis of Solid Teflon Pulsed Plasma Thruster," *Journal of Spacecraft*, Vol. 7, No. 12, 1970, pp. 1402–1406.

[7]Vondra, R. J., and Thomasson, K. I., "Performance Improvements in Solid Fuel Microthrusters," *Journal of Spacecraft*, Vol. 9, No. 10, 1972, pp. 738–742.

[8]Spanjers, G. G., McFall, K. A., Gulczinski, F. S., and Spores, R. A., "Investigation of Propellant Inefficiencies in a Pulsed Plasma Thruster," AIAA Paper 96-2723, July 1996.

[9]Spanjers, G. G., Lotspeich, J. S., McFall, K. A., and Spores, R. A., "Propellant Losses Because of Particulate Emission in a Pulsed Plasma Thruster," *Journal of Propulsion and Power*, Vol. 14, No. 4, 1998, pp. 554–559.

[10]Haag, T. W., "PPT Thrust Stand," AIAA Paper 95-2917, July 1995.